CFD simulations of gas-liquid-liquid three-phase co-current flow in horizontal pipe by tracking volume fractions using VOF model

Muhammad Waqas Yaqub and Rajashekhar Pendyala*

Chemical Engineering Department, Universiti Teknologi PETRONAS, 32610 Seri Iskandar, Perak Darul Ridzuan, Malaysia.

*Corresponding author: rajashekhar_p@utp.edu.my

Abstract. The gas-liquid-liquid three-phase co-current flow is frequently observed in upstream petroleum pipelines. The identification of three-phase flow patterns is important to characterize three-phase flow dynamics. The three-phase flow patterns change with the pipe diameter, superficial velocities and physical properties of the fluids. Computational fluid dynamics (CFD) analysis of three-phase flow through 0.1524 m diameter and 3.5 m long horizontal pipe has been conducted. The superficial velocity ranges of gas-oil-water were 0.5-4, 0.08-0.32 and 0.08-0.32 m/s respectively. The volume of fluid (VOF) model was used to simulate the three-phase interfacial structures. According to the results, the three-phase flow patterns have been successfully simulated. Three-phase flow regime map has been constructed to analyze the flow pattern transition with the superficial velocities. The three-phase flow pressure drop increased with the superficial velocities of oil and water. However, the drop in pressure first increased and then decreased with the increase in superficial velocity of the gas.

1. Introduction
The fluid mixture produced from petroleum reservoirs mainly consists of gas, crude oil, and water. This fluid mixture is transported to the processing facilities through pipelines. Thus, gas-oil-water flow co-currently in upstream pipelines. Three-phase flow dynamics such as pressure drop, liquid holdup, and volumetric phase fractions are associated with the flow pattern. The liquid holdup and pressure drop are the common flow assurance problems. Various studies have been conducted to identify three-phase flow patterns. Three-phase flow patterns are differentiated based on gas-liquid and liquid-liquid interfacial relationship. Commonly occurring gas-liquid flow patterns are annular, plug, churn, slug, and stratified flow [1-4]. The oil-water could flow in the form of separate layers or as a homogeneous liquid mixture or one liquid as a continuous phase and the other one as dispersed phase [5, 6].

The three-phase flow pattern is the function of the diameter of the pipe, superficial velocities and physical properties of the fluids. The pipe diameter significantly influences the three-phase flow pattern and resultant pressure drop. Increase in the pipe diameter decreases the flow velocity which leads to the reduced pressure drop [7]. Some studies on three-phase flow to identify the flow patterns and the pressure drop are available in the literature. However, most of the previous studies were conducted with the small diameter pipes. The size of the commercial scale pipes is much bigger than laboratory scale pipes used in experiments for the identification of flow pattern. Therefore, the identification of realistic flow patterns and pressure drop is needed. The advancement in the processing ability of computers has made the CFD, a robust tool to study the flow dynamics in the desired range of parameters and geometries. The CFD analysis on two-phase flow has been carried out by Ekambara et al. [8], Bramara et al. [9] and Mazumder et al. [10]. However, the CFD analysis of three-phase flow in pipes is not available in the literature. The analysis was intended to simulate the

three-phase flow patterns in the 0.1524 m internal diameter horizontal pipe at various gas, oil, and water superficial velocities.

2. Methodology

2.1. Geometry and Meshing
The geometry of the pipe was created in the Ansys design modeler tool. The length and internal diameter (ID) of the pipe were 3.5 m and 0.1524 m respectively. The minimum pipe length to diameter ratio (L/D) for turbulent flow to get the fully developed velocity profile was 10 [11] and the L/D ratio of the created pipe geometry has the (L/D) ratio of 23 to ensure the fully developed flow and to study the variations of flow parameters after the flow developing length as shown in Figure 1 (a). The results of CFD analysis strongly depends on the type of mesh employed [12]. The structured hexahedral mesh was preferred due to improved orthogonal quality and lower skewness as shown in Figure 1 (b). The mesh independence analysis was conducted at four different number of mesh cells by plotting the maximum absolute pressure for each mesh as shown in Figure 2.

(a)

(b)
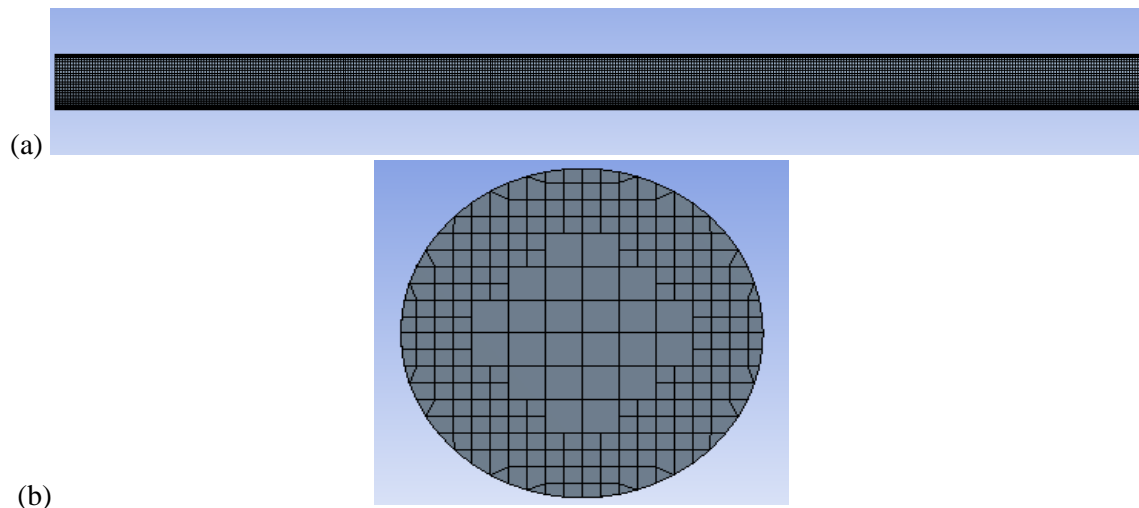
**Figure 1. (a)** Meshed horizontal pipe geometry, **(b)** Cross section view of the pipe mesh.

2.2. Boundary conditions and physical properties of fluids
The appropriate boundary conditions were chosen for a practical solution. The physical properties of the phases are given in table 1. The operating gauge pressure was set at zero as the flow system was considered to run at atmospheric pressure (101.32 *kPa*). The walls of the flow domain were considered to have no-slip condition and wall roughness was set as a smooth wall. The mixture velocity was given at the inlet according to the different set of superficial velocities in table 2. The volumetric phase fractions of oil and water based on the superficial velocities of each phase is calculated and specified at the inlet given in table 2. Air was declared as primary phase due to its higher phase fraction compared to other phases. Total 20 different combinations of gas-oil-water have been simulated to analyze the change in flow patterns from low to high superficial velocities. The surface tension effect was neglected due to the higher inertial forces than the surface tension force described by Weber number more than 1 [13].

2.3. Multiphase model
The volume of fluid VOF has been used to reveal the interfacial relationship between the phases. The VOF model solves a set of momentum equation to model the flow of immiscible fluids. The VOF model can model two or more immiscible fluids by the solution of a single set of momentum

equation. The implicit body force was used to include the gravitational effect in the flow along Y-axis. The momentum equation for VOF model is given in equation (1) [13].
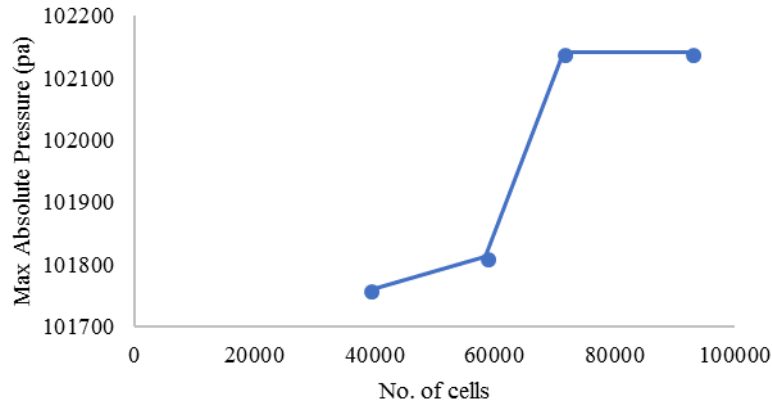
Figure 2. Mesh sensitivity analysis

Table 1. Physical properties of fluids

Sr No.	Name	Phase	Density (kg/m^3)	Viscosity (kg/m·s)
1	Air	Gas	1.225	0.00001789
2	Oil	Liquid	840	0.0084
3	Water	Liquid	1000	0.001

$$\frac{\partial}{\partial t}(\rho \bar{v}) + \nabla.(\rho \bar{v}\bar{v}) = -\nabla p + \nabla.[\mu.(\nabla \bar{v} + \nabla \bar{v}^T)] + \rho \bar{g} + \bar{F}$$

(1)

Where g and t are the acceleration due to gravity and time respectively and ρ, p, μ and v are the density, pressure, dynamic viscosity and velocity of the phase k respectively. The term T is the stress tensor and F is the external force. The continuity equation for the volumetric fraction of one or more phases is given as.

$$\frac{1}{\rho_q}\left[\frac{\partial}{\partial t}(\alpha_q \rho_q) + \nabla.(\alpha_q \rho_q \bar{\mathcal{V}}_q) = S_{\alpha q} + \sum_{p=1}^{n}(\dot{m}_{pq} - \dot{m}_{qp})\right]$$

(2)

Where, a and ρ are the volume fraction and density of the qth phase respectively and t is the time. The source term is zero by default is S_{aq}. The transfer of mass p to q and from q to p are denoted by term $\dot{m}_{pq}$ and $\dot{m}_{qp}$ respectively.

2.4. Turbulence model

The flow conditions adopted in the flow domain clearly indicates the occurrence of turbulence in the flow. Therefore, the simulation of turbulence was necessary to get the accurate results. The *k-epsilon* turbulence model was used, which is described by the following equations [14].

$$\rho v_j \frac{\partial k}{\partial x_j} = \frac{\partial}{\partial x_j}\left(\frac{\mu_t}{\sigma_k}\frac{\partial k}{\partial x_j}\right) + \mu_t \frac{\partial v_j}{\partial x_i}\left(\frac{\partial v_i}{\partial x_j} + \frac{\partial v_j}{\partial x_i}\right) - \rho \varepsilon$$

(3)

$$\rho v_j \frac{\partial \varepsilon}{\partial x_j} = \frac{\partial}{\partial x_j}\left(\frac{\mu_t}{\sigma_\varepsilon}\frac{\partial \varepsilon}{\partial x_j}\right) + C_1 \mu_t \frac{\partial v_j}{\partial x_i}\left(\frac{\partial v_i}{\partial x_j} + \frac{\partial v_j}{\partial x_i}\right) - C_2 \frac{\varepsilon}{k}\rho \varepsilon$$

(4)

Where, k represents the turbulent kinetic energy and the dissipation rate of k is denoted by ε. $C1$, $C2$, σ_ε, and σ_k are constants.

2.5. Solver and time step

Pressure based solver has been used. The algorithm used for the solution of Navier-Stokes equations was SIMPLE. The second-order upwind scheme was used for solving the momentum equation and

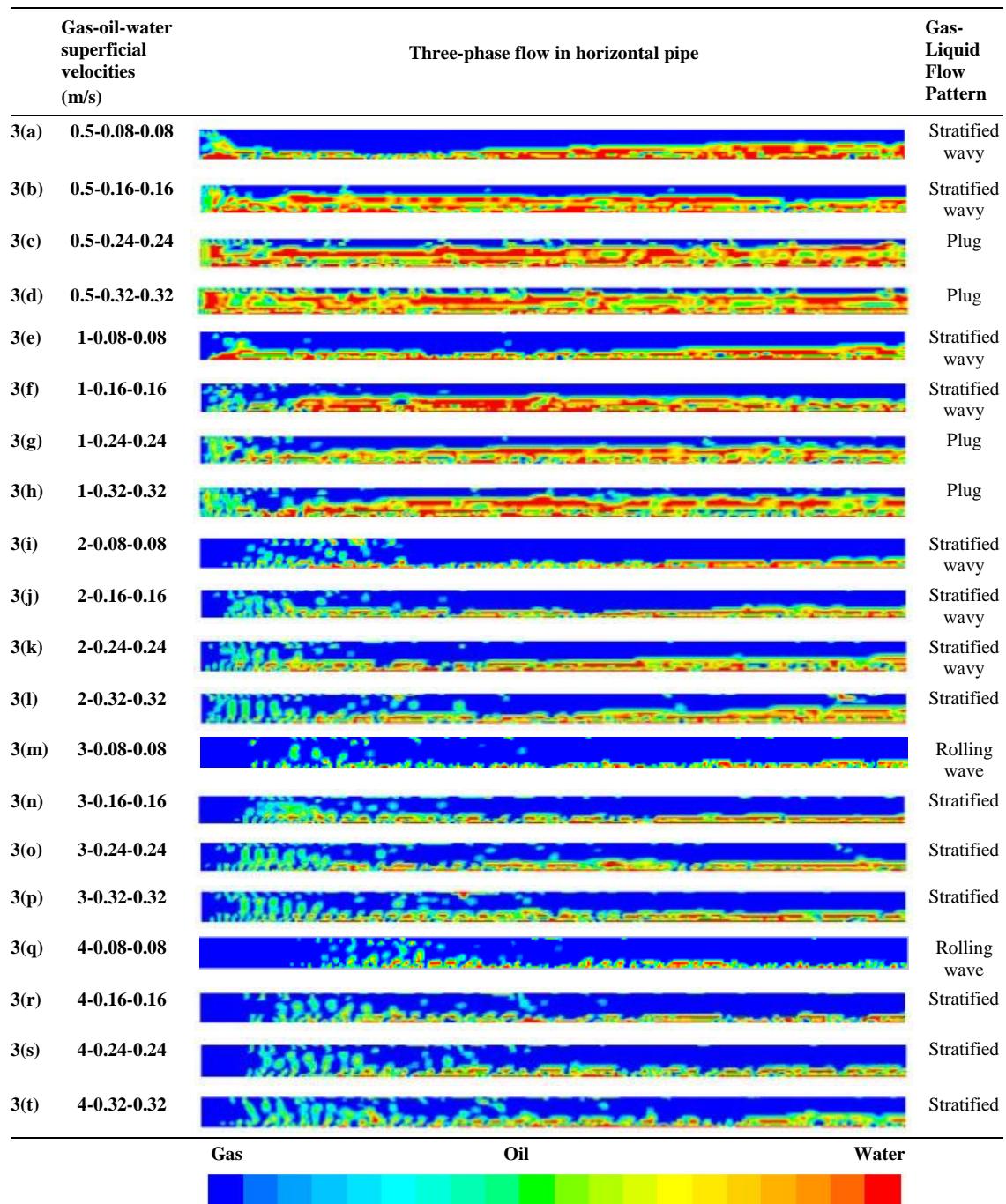**Table 2.** Superficial velocities and volume fractions of fluids

	Gas superficial velocity (m/s)	Oil Superficial velocity (m/s)	Water superficial velocity (m/s)	Mixture velocity (m/s)	Oil volume fraction	Water volume fraction
1	0.5	0.08	0.08	0.66	0.121	0.121
2	1	0.08	0.08	1.16	0.068	0.068
3	2	0.08	0.08	2.16	0.037	0.037
4	3	0.08	0.08	3.16	0.025	0.025
5	4	0.08	0.08	4.16	0.019	0.019
6	0.5	0.16	0.16	0.82	0.195	0.195
7	1	0.16	0.16	1.32	0.121	0.121
8	2	0.16	0.16	2.32	0.074	0.074
9	3	0.16	0.16	3.32	0.048	0.048
10	4	0.16	0.16	4.32	0.037	0.037
11	0.5	0.24	0.24	0.98	0.244	0.244
12	1	0.24	0.24	1.48	0.162	0.162
13	2	0.24	0.24	2.48	0.096	0.096
14	3	0.24	0.24	3.48	0.068	0.068
15	4	0.24	0.24	4.48	0.053	0.053
16	0.5	0.32	0.32	1.14	0.280	0.280
17	1	0.32	0.32	1.64	0.195	0.19
18	2	0.32	0.32	2.64	0.121	0.121
19	3	0.32	0.32	3.64	0.087	0.087
20	4	0.32	0.32	4.64	0.068	0.068

Geometric reconstruction scheme was used to solve volume fraction equations to minimize numerical diffusion. Transient calculations were conducted to analyze the change in interface structure between the phases with the time. VOF model gives an excellent feature of the variable time step, which increases or decreases the time step size with the change in the size of the cell to meet the global courant number criteria. Thereby, decreases the computational time. The simulations were conducted for 8 seconds to allow the flow to become completely stable.
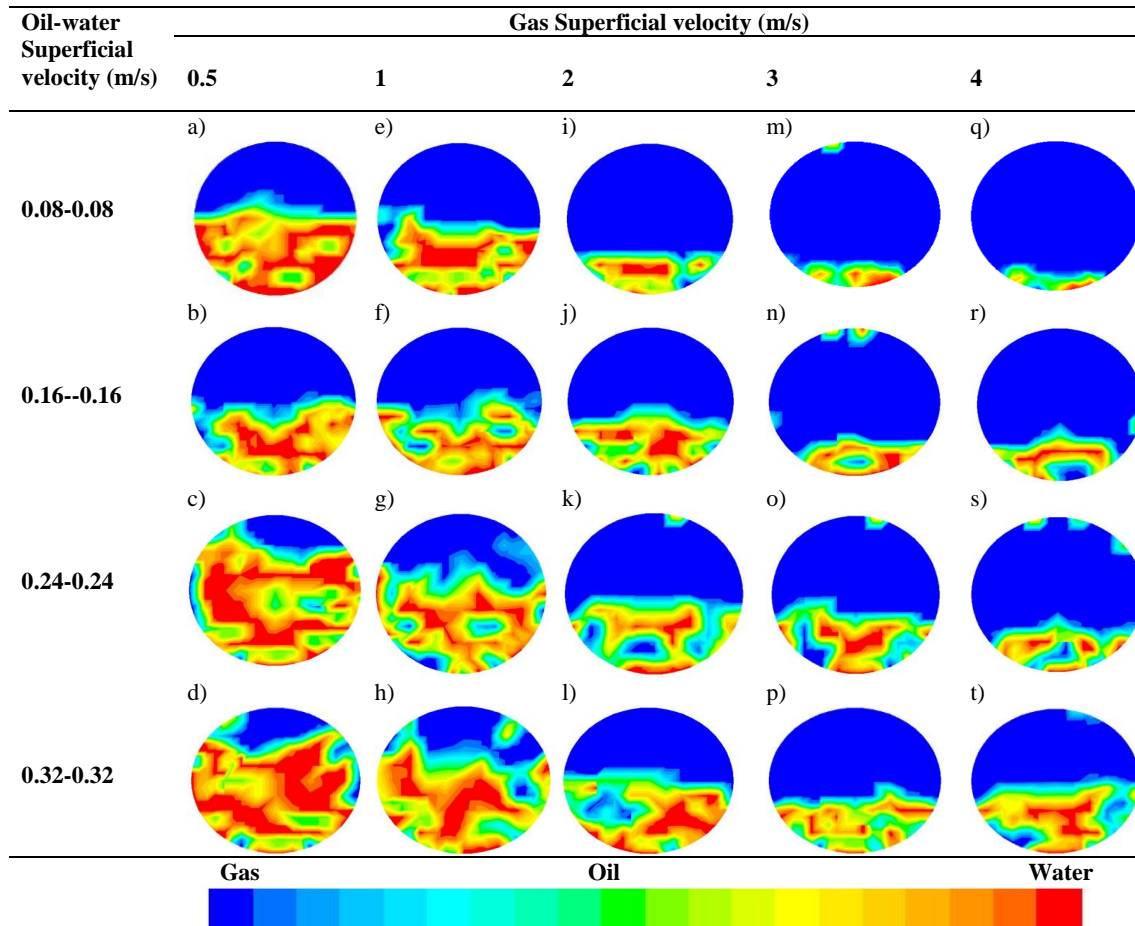
3. Results and Discussion

3.1. Three-phase flow patterns

The contours of three-phase horizontal flow in the pipe along the X-Y plane is shown in Figure 3. Three-phase plug, stratified, stratified wavy and stratified rolling wave flow patterns have been observed. Intermittent plugs of gas and liquid were moving in the upper section of the pipe as shown in the contours of plug flow in Figure 3. Most of the pipe cross-section was filled with the liquid because of the high volumetric phase fractions of oil and water. In such conditions where the volumetric fraction of gas is lower than the total liquid volume fraction, the gas phase is driven by the liquid phase [3]. At low gas superficial velocity, the oil and water were not completely mixed during plug flow as shown by the cross-section Figure 4 (c) and (d). However, increase in superficial velocity of gas increased the oil-water mixing shown in Figure 4 (g) and (h). According to the simulation results, the stratified flow was the highly occurring flow pattern in three-phase co-current horizontal flow in the pipe. The gas-liquid interface was straight and smooth. During stratified flow, liquid phases flow in separate layers or in the form of a mixture as shown in

	Gas-oil-water superficial velocities (m/s)	Three-phase flow in horizontal pipe	Gas-Liquid Flow Pattern
3(a)	0.5-0.08-0.08		Stratified wavy
3(b)	0.5-0.16-0.16		Stratified wavy
3(c)	0.5-0.24-0.24		Plug
3(d)	0.5-0.32-0.32		Plug
3(e)	1-0.08-0.08		Stratified wavy
3(f)	1-0.16-0.16		Stratified wavy
3(g)	1-0.24-0.24		Plug
3(h)	1-0.32-0.32		Plug
3(i)	2-0.08-0.08		Stratified wavy
3(j)	2-0.16-0.16		Stratified wavy
3(k)	2-0.24-0.24		Stratified wavy
3(l)	2-0.32-0.32		Stratified
3(m)	3-0.08-0.08		Rolling wave
3(n)	3-0.16-0.16		Stratified
3(o)	3-0.24-0.24		Stratified
3(p)	3-0.32-0.32		Stratified
3(q)	4-0.08-0.08		Rolling wave
3(r)	4-0.16-0.16		Stratified
3(s)	4-0.24-0.24		Stratified
3(t)	4-0.32-0.32		Stratified

Gas   Oil   Water

Figure 3. Contours of the X-Y plane of the horizontal pipe

Oil-water Superficial velocity (m/s)	Gas Superficial velocity (m/s)				
	0.5	1	2	3	4
0.08-0.08	a)	e)	i)	m)	q)
0.16--0.16	b)	f)	j)	n)	r)
0.24-0.24	c)	g)	k)	o)	s)
0.32-0.32	d)	h)	l)	p)	t)

Gas   Oil   Water

Figure 4. Contours of cross-section of three-phase flow in horizontal pipe

the contours of the cross-section in Figure 4. The three-phase stratified flow can be further subdivided based on the changes occur at the gas-liquid interface at various superficial velocities of fluids. In stratified wavy flow, the gas-liquid interface has the wave-like appearance as shown in Figure 3.

The stratified wavy flow pattern observed at low and moderate superficial velocities of gas and liquids. The pressure exerted by the gas on the liquid surface tends to push the liquids in the forward direction, which resulted in the creation of waves at the gas-liquid interface. The oil-water were flowing in the separate layers during the stratified wavy flow pattern at low superficial velocities of gas and liquids. However, the liquid layer changed to mixture flow with the increase in the superficial velocities of gas and liquids as shown by the cross-section contours in Figure 4. At a high superficial velocity of the gas and low superficial velocities of liquids, the stratified wavy flow pattern changed into the stratified rolling waves. This is due to the increase in pressure of gas at the interface, at which the interfacial waves changed to the rolling waves. Thereby created splashes at the gas-liquid interface. At high gas superficial velocity, more turbulence was induced in the liquid phases, which made a homogeneous mixture as shown in Figure 4 (k), (l), (o), (p) and (s).

3.2. Flow regime map

The flow regime map indicating three-phase flow patterns at various superficial velocities of gas and liquids is shown in Figure 5. At low gas and liquid superficial velocity, the gas-liquid adopted stratified wavy interface. Plug flow has been observed at low gas and high liquid superficial velocity. At a moderate superficial velocity of the gas, increase in the superficial velocity of the total liquid, shifted the stratified wavy flow to smooth stratified flow. Increase in the superficial velocity of the gas at a low superficial velocity of liquid changed the flow from stratified wavy to rolling wave. At high superficial velocities of gas and liquids, the flow pattern was smooth stratified. Separate layers of oil and water were observed at low superficial velocities of gas and liquids. Increase in the superficial velocities of gas and liquid increased the mixing in the liquid phase, due to which a complete homogeneous oil-water mixture was obtained. The three-phase flow regime map of Lee et al. [3] with 0.1 m internal diameter pipe showed that the stratified flow only occurred at low gas and liquid velocities. However, the comparison shows that the slug flow in Lee et al. [3] map is replaced by the stratified flow. The replacement of slug flow by smooth stratified flow is due to the increase in the diameter of the pipe as compared to the pipe used in the work of Lee et al. [3].
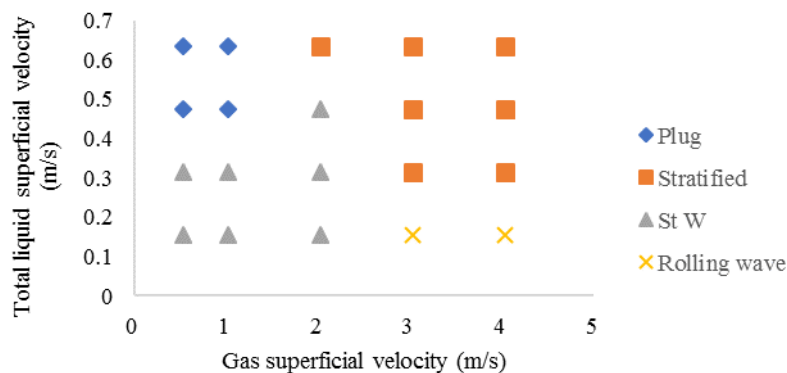
Figure 5. Three-phase horizontal flow regime map

3.3. Pressure drop

According to the literature, the pressure drop increased with the increase in superficial velocities of gas and liquid [15, 16]. The effect of gas on pressure drop was more profound than the liquid phases [17]. However, the trend of the pressure drop with the increase in the gas flow rate was slightly different as shown in Figure 6. The pressure drop increased with the superficial velocities of liquid. However, the pressure drop first increased with superficial velocity of the gas and then started decreasing with further increase in superficial velocity of the gas. This behavior is described by the governing flow pattern at respective superficial velocity of the gas. The pressure drop increased up to the gas superficial velocity of 2 m/s. The flow pattern at this superficial velocity was stratified wavy.
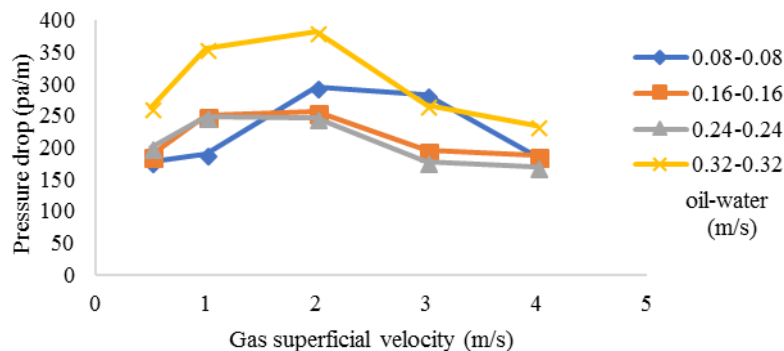
Figure 6. Variation of pressure drop with the gas velocity at different oil-water velocities

The reduction in pressure drop occurred when the type of flow pattern shifted from stratified wavy to smooth stratified flow at high superficial velocities of gas and total liquid. The pressure drop was reduced to almost initial level when the flow pattern is smooth stratified. At high superficial velocities of gas and total liquid, the momentum of the fluids was high enough to minimize the slip between the phases. The reduced slip, and smooth gas-liquid interface in stratified flow resulted in the reduced pressure drop.

4. Conclusions

CFD simulations of three-phase flow through a 0.1524 m diameter pipe were conducted. The superficial velocity ranges of gas-oil-water were 0.5-4, 0.08-0.32 and 0.08-0.32 m/s respectively. The flow patterns at various superficial velocities have been successfully simulated with VOF model. The observed flow patterns were stratified, stratified wavy, stratified rolling wave and plug flow. The flow regime map has been constructed to analyze the flow regime transition with the superficial velocities of fluids. Pressure drop increased with the increase in superficial velocity of liquids. However, pressure drop first increased and then decreased with increase in the gas flow rate. This behavior is because of following flow pattern at the given superficial velocities of fluids. The pressure drop increased due to the plug and stratified wavy flow and then decreased when the flow pattern changed to smooth stratified flow.

Acknowledgment

References

[1]   Açikgöz M, Franca F and Lahey R 1992 An experimental study of three-phase flow regimes *Int. J. Multiphase Flow* **18**(3) 327

[2]   Woods G et al. 1998 Three-phase oil/water/air vertical flow *Chem. Eng. Res. Des*. **76**(5) 571

[3]   Lee A, Sun J and Jepson W 1993 Study of flow regime transitions of oil water-gas mixtures in horizontal pipelines. in *The Third International Offshore and Polar Engineering Conference*. International Society of Offshore and Polar Engineers

[4]   Qiang W et al. 2016 Experimental tomographic methods for analysing flow dynamics of gas-oil-water flows in horizontal pipeline *J. Hydrodyn.* Ser. B **28**(6) 1018

[5]   Keskin C, Zhang H Q and Sarica C 2007 Identification and Classification of New Three-Phase Gas/Oil/Water Flow Patterns. in *SPE Annual Technical Conference and Exhibition*. Society of Petroleum Engineers.

[6]   Spedding P, Donnelly G and Cole J 2005 Three phase oil-water-gas horizontal co-current flow: I. Experimental and regime map *Chem. Eng. Res. Des.* **83**(4) 401

[7]   Cimbala J M and Çengel Y A 2014 *Fluid mechanics: fundamentals and applications*.

[8]   Ekambara K et al. 2008 CFD simulation of bubbly two-phase flow in horizontal pipes *Chem. Eng. J.* **144**(2) 277

[9]   Bhramara P et al. 2009 CFD analysis of two phase flow in a horizontal pipe–prediction of pressure drop *Momentum* **10** 476

[10]   Mazumder Q H and Siddique S A 2011 CFD analysis of Two-phase Flow Characteristics in a 90 degree Elbow. *The J. of Comp. Multiphase Flows* **3**(3) 165

[11]   Bergman T L and Incropera F P 2011 *Fundamentals of heat and mass transfer* John Wiley & Sons.

[12]   Hernandez-Perez V, Abdulkadir M and Azzopardi B 2011 Grid generation issues in the CFD modelling of two-phase flow in a pipe T*he J. of Comp. Multiphase Flows* **3**(1) 13

[13]   Fluent A 2013 *ANSYS fluent theory guide* 15.0. Inc, Canonsburg, PA

[14]   Launder B E and Spalding D B 1972 *Mathematical models of turbulence* Academic press.

[15]   Wang H Q, Wang Y and Zhang L 2011 Characteristics of pressure gradient fluctuation for oil-gas-water three-phase flow based on flow pattern. in *App. Mechs. and Mat*. Trans Tech Publ.

[16]   Shmueli A, Unander T and Nydal O 2015 Characteristics of Gas/Water/Viscous Oil in Stratified-Annular Horizontal Pipe Flows. in OTC Brasil *Offshore Technology Conference*

[17]   Bannwart A et al. 2009 Experimental investigation on liquid–liquid–gas flow: flow patterns and pressure-gradient *J. of Pet. Sci and Engg* **65**(1) 1